

NCT at the MEPHI reactor

K. Zaitsev¹, A. Portnov¹, V. Sakharov¹, V. Troshin¹, V. Savkin¹, V. Kvasov¹, O. Mishcherina¹,
V. Kulakov², V. Khokhlov², I. Sheino², V. Meshcherikova³, V. Mitin³, N. Kozlovskaya³,
I. Shikunova³

¹*Moscow Engineering Physics Institute (State University) - MEPHI*

²*State Research Center – Institute of Biophysics*

³*Russian Cancer Research Center of the Russian Academy of Medical Science*

Introduction

For many various forms of cancer diseases, conventional methods of treatment are ineffective. Enormous funds have been spent on improvement of chemotherapy, immunotherapy, and radiotherapy methods; however, still nearly half of the patients die. The therapeutic efficiency may be increased with a method that provides selective damage of the tumor, saving normal tissue cells. Neutron capture therapy (NCT) is this method. The essence is simple: a compound containing boron, gadolinium or other elements with large thermal neutron capture cross-section is administered into the tumor. As a result of the thermal neutron capture in the tumor, secondary radiation occurs, which damages the tumor cells. Therefore, NCT is intensively developed all over the world.

Materials and Methods

In 1993, first NCT experiments [1] were carried out at the MEPHI reactor (fig. 1) with use of the drug Magnevist (manufactured by Schering). Magnevist is a contrast agent in NMR diagnostics of brain tumors, i.e. it is capable of accumulating in tumor tissues. White rats with inoculated tumors (Ensen sarcoma and C-45 sarcoma) were used as tumor-carrying animals. The drug Magnevist was administered directly into the tumor. In the experiments, initial concentration of the drug and time of irradiation were selected so that the tumors exhibited resorption in 80% of rats with the drug (fig. 2).

Inspired by the first results [2-7], the team of scientists representing MEPHI, SSC Institute of Biophysics, Russian Cancer Research Centre of RAMS, etc., set the task to create a clinical base in Moscow for new radiation technologies of radiotherapy of malignant tumors on the basis of the



Fig. 1. MEPHI reactor: a 2.5 MW water-moderated pool-type reactor with a beryllium-water reflector, with 10 horizontal and 20 vertical channels. Thermal neutron flux in the reflector is 4.0×10^{13} n/cm²/s.

MEPhI nuclear reactor [8], and to introduce the NCT method in clinical practice in order to increase the efficiency of treatment of malignant neoplasm, which are poorly cured or incurable with conventional methods.

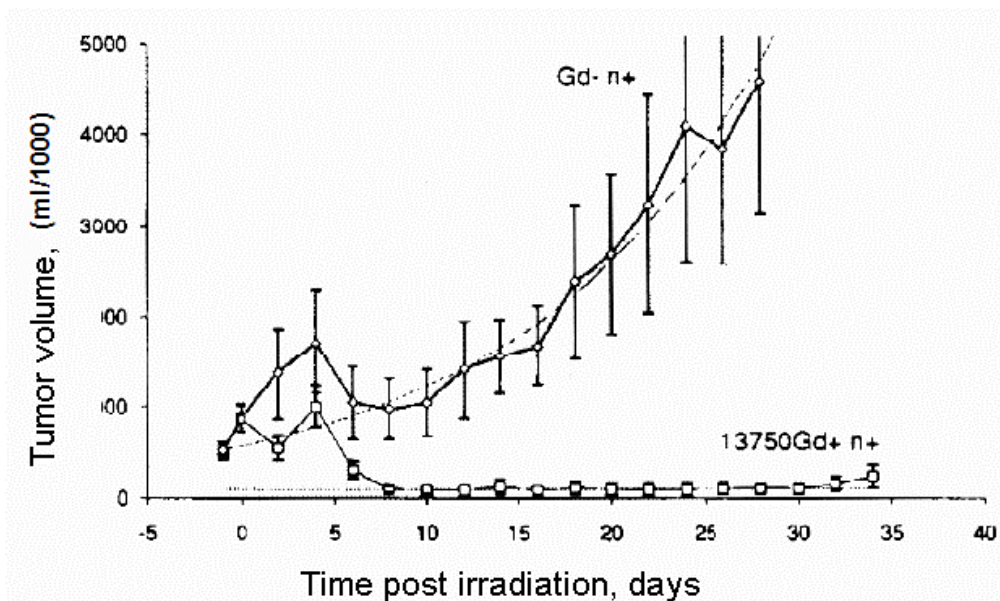


Fig. 2. Tumor growth dynamics in rats post irradiation [1] without the compound (1) and with the compound (2).

The primary purpose of work is carrying out complex preclinical studies on the NCT technology at the MEPhI nuclear reactor. Thus, the strategic direction of research has been chosen, which in the shortest time will allow to apply the new NCT-based radiation technology in practice, i.e. to treat malignant tumors taking into account our conditions and opportunities. The shortest way is treating malignant melanoma, since the thermal neutron beam available at the MEPhI reactor allows treating effectively only tumors localized close to the body surface, since the thermal neutron flux decreases half the value at a depth of ~ 3 cm. Malignant melanoma is a skin cancer; the incidence rate of melanoma approach the epidemic scale. Malignant melanoma is a highly lethal disease resistant to the conventional radiological methods of treatment.

The implementation of the NCT method requires a beam with maximum thermal neutron flux and low content of background photons and fast neutrons. The tangential horizontal experimental channel HEC-4 of 150 mm in diameter meets these requirements to the highest extent.

A characteristic feature of the tangential channels of nuclear reactors is that their axis is out of the core, which is a source of fast neutrons and gamma-rays. Therefore, the latter come to the outlet of the tangential channel only after scattering, unlike the radial channel, at the outlet of which there are both scattered and non-scattered radiations. Naturally, the admixture of fast neutrons and photons at the outlet of the tangential channel is lower than that in the radial channel.

With the purpose of creation of an irradiation room on the channel HEC-4, the reactor channels were reconstructed. Fig. 3 shows a schematic of the redesign.

Calculations and experimental studies have been carried out on optimization of the intrachannel devices (scatterers, collimators, filters, diaphragms, etc.) and their influence on formation of the radiation field at the outlet of the channel, in order to achieve its optimum characteristics; appropriate design solutions were proposed.

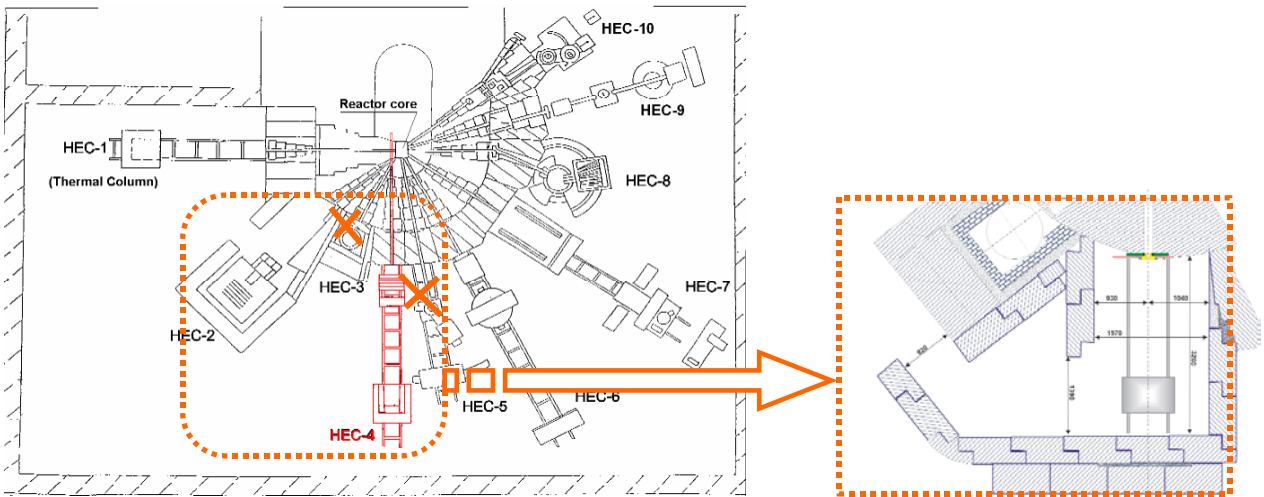


Fig. 3. Redesign of the reactor channels.

In order to increase the intensity of thermal neutrons, to soften the neutron spectrum, decrease the fraction of photons and fast neutrons in relation to the thermal neutron flux in the tangential channel, a graphite scatterer was installed opposite to the core. The photon flux outgoing from the channel was attenuated using a filter from polycrystalline bismuth placed in the aluminum cylinder. To decrease the background, the thermal neutron beam was formed with conic collimators. Thus was increased the luminous spot and the area of the inner surface of the collimators, from which the scattered neutrons are collected.

In accordance with the developed engineering requirements and the drawings, the intrachannel devices were reconstructed, including: the graphite scatterer, shutter device, lead collimator with bismuth inserts (fig. 4). The outlet aperture of the collimator is surrounded with lithium-containing material (${}^6\text{Li}$).

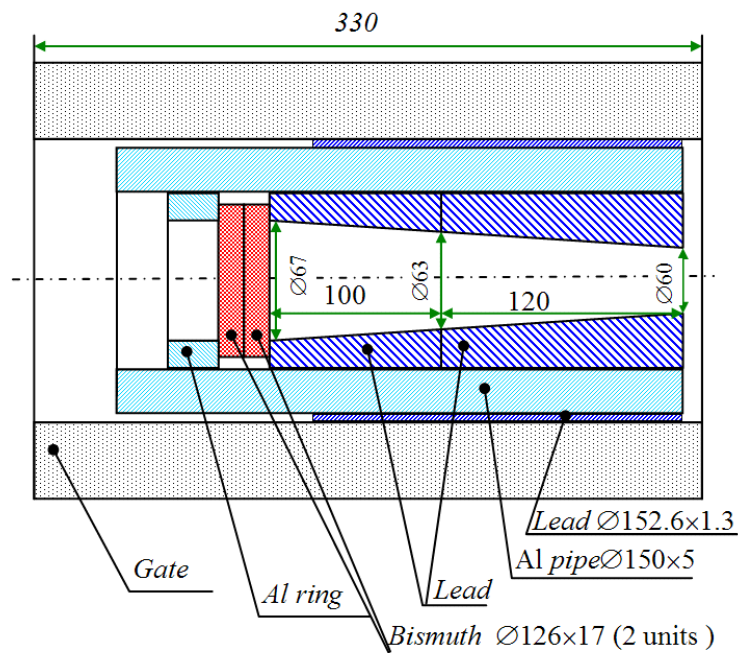


Fig. 4. Collimator in the first section of the shutter.

The reconstruction of the channel resulted in the following characteristics of the neutron beam:

- Beam diameter: 30÷60 mm;
- Thermal neutron flux: 10^9 neutron/cm²·s;
- Fast neutron dose per thermal neutron: $4.7 \cdot 10^{-11}$ cGy·cm²/n;
- Photon dose rate in the beam: 0.025 cGy/s.

The neutron beam of the reactor is extended into a specially designed and built irradiation room. The walls of the room consist of monolithic concrete blocks, the locking configuration of which allows avoiding direct "shots" of radiations, a layer of lead bricks and blocks of borated lead-containing polyethylene; the room has a labyrinth entrance made of concrete blocks. Fig. 5 shows the external side of the irradiation room.

The inner size of the room is: length - 3200 mm, width - 1970 mm, height - 2170 mm. These dimensions of the room will allow performing experimental studies in animals of any sizes (fig. 6).

The whole internal surface of the irradiation room is covered with borated polyethylene with lead. The surface around the beam outlet aperture is additionally covered with a plate of lithium-containing material enriched in the isotope ⁶Li. The biological protection of the irradiation room meets the standards of radiation safety for the personnel.

The room is equipped with a movable bench for the experimental animals. Inside the room (fig. 7.), on the floor there are rails for the trolley that is rigidly connected to the bench for fixing an object for irradiation. The bench size is 510 × 800 mm, and the whole system has three degrees of freedom.



Fig. 5. Irradiation room.



Fig. 6. Preparation of the animal for irradiation in the room.



Fig. 7. The system to guide the neutron beam of the reactor into the irradiation room, and a movable platform to fix experimental animals.

The vital functions of the animal during an NCT session are maintained using communication lines through the concrete protection to a dropper, and a device for the control of physiological parameters was set up inside the room in a special compartment separated from the irradiation chamber (fig. 8). The animal, and readings of the device for the control of physiological parameters were observed during the NCT session by means of two tiny video cameras transmitting the image to a monitor (fig. 9):



Fig. 8. Device for the control of physiological parameters.



Fig. 9. Video monitors.



Fig. 10. Optical laser at the channel outlet.

The video monitors and the power supply of the camera are installed on the 2nd floor of the reactor. The cable communication line is laid between the room and the table with video control devices. In order to maintain normal air flow and temperature, warm air is forced into the room. The adjustment of the object to be irradiated relative to the neutron beam axis is done using an optical laser. (Fig. 10).

The body of the animal was protected with a soft shield with ${}^6\text{Li}$ (fig. 11).



Fig. 11. Shielding of normal tissues using soft ${}^6\text{Li}$ -containing material.

Dosimetry

During irradiation, dosimetry of photon and neutron radiation is performed.

The dosimetry of photons during irradiation was carried out using PST detectors (the glass IS-7) from the complete set IKS, and for neutrons - PST-L from the glass 540-1 enriched in ${}^6\text{Li}$, and gold foils. The geometrical center of the beam was determined and controlled by means of x-ray films such as RM-1. Fast neutrons were registered using activation detectors with the nuclides ${}^{32}\text{S}$ and ${}^{69}\text{Cu}$.

A method of direct biological dosimetry with use of tumor cell suspension cultures was developed and implemented, which proved practical efficiency in verification of the results of biological dosimetry of mixed neutron-photon fields. The results of biological dosimetry coincide with the evaluation based on physical dosimetry methods of and accepted by us for the calculation of data on relative biological efficiency (RBE) [9].

Compounds

The NCT technology is developed using drugs with ^{10}B and Gd.

Boron and gadolinium used in the compounds in the NCT technology create secondary radiation of different nature in the tumor. Fig. 12 shows the relevant nuclear reactions. It is obvious that all secondary radiation of the ^{10}B reaction is localized within the site of its location. The range of decay products is 5 - 9 μm . The reaction on ^{157}Gd produces rather hard photon radiation and electron radiation (conversion and Auger electrons). The latter, with a range of 1 - 40 μm , is localized in the site of gadolinium distribution.

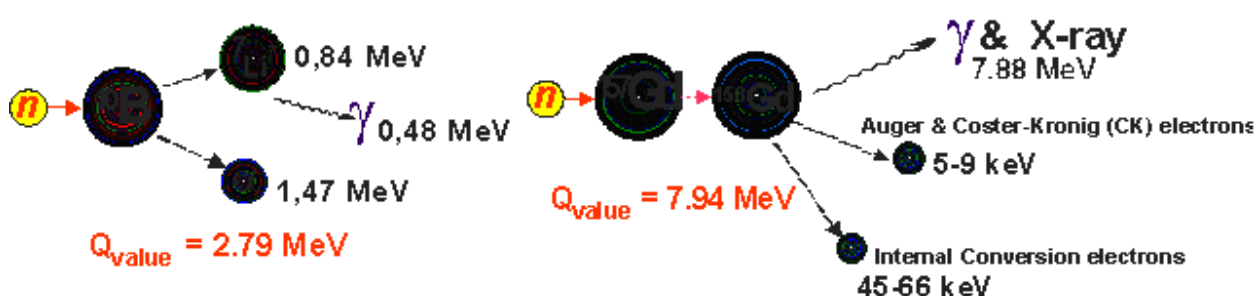


Fig. 12. Nuclear reactions used in NCT.

We estimated the spectrum of electrons and photons of the thermal neutron capture reaction $^{157}\text{Gd}(n,\gamma)$. The estimated values of the photon spectrum for this reaction obtained by J. Stepanek at al. [10], C Wang [11], T. Goorley at al. [12] with processing of the file ENSDF, contain no data on photon emission in the range of 2.1 MeV to 3.7 MeV. The total energy of photons is $\sim 2.2 \text{ MeV}$, which is essentially below the excitation energy of ^{158}Gd $Q=7.94 \text{ MeV}$. Our estimations of the photon spectrum are based on the results of J. K. Tuli [13] for lines and data of L. Groshev at al. [14] for continuous component spectra. For the first time we managed to obtain a photon spectrum preserving the balance of total excitation energy of the ^{158}Gd nucleus (fig. 13).

Basing on the data obtained with use of the library JENDL-3.3 of cross-sections for the reaction of radiation capture, elastic and inelastic scattering of neutrons on nuclei of all nuclides included in the natural mixture of gadolinium isotopes, dependence of specific kerma of Gd-nat neutrons vs energy was calculated.

The estimation of energy dependence of specific kerma of neutrons for soft biological tissue in comparison with the same data for neutron capture agents at a ^{10}B concentration of 35 ppm and Gd-nat - 5500 ppm are shown in fig. 14. The dependence of specific kerma of ^{10}B vs. energy was obtained from R.G. Zamenhof at al. [15].

The data represented show that the additional energy release in the biological tissue at the expense of gadolinium and boron can vary essentially depending on the working neutron spectrum in the energy region $<1 \text{ eV}$.

The mechanisms underlying the damage of tumor cells for the use of L-BPA and Dipentast in NCT are different. According to Y. Mishima [16], the enzyme systems responsible for the synthesis of melanin pigment in melanoma cells fail to distinguish the molecules of L-phenylalanine and ^{10}B -boron-L-phenylalanine. As a result, the atoms of ^{10}B appear inside the tumor cells. When the gadolinium-containing drug Dipentast is used, gadolinium does not penetrate into the tumor cells, and it is located only in the intercellular space.

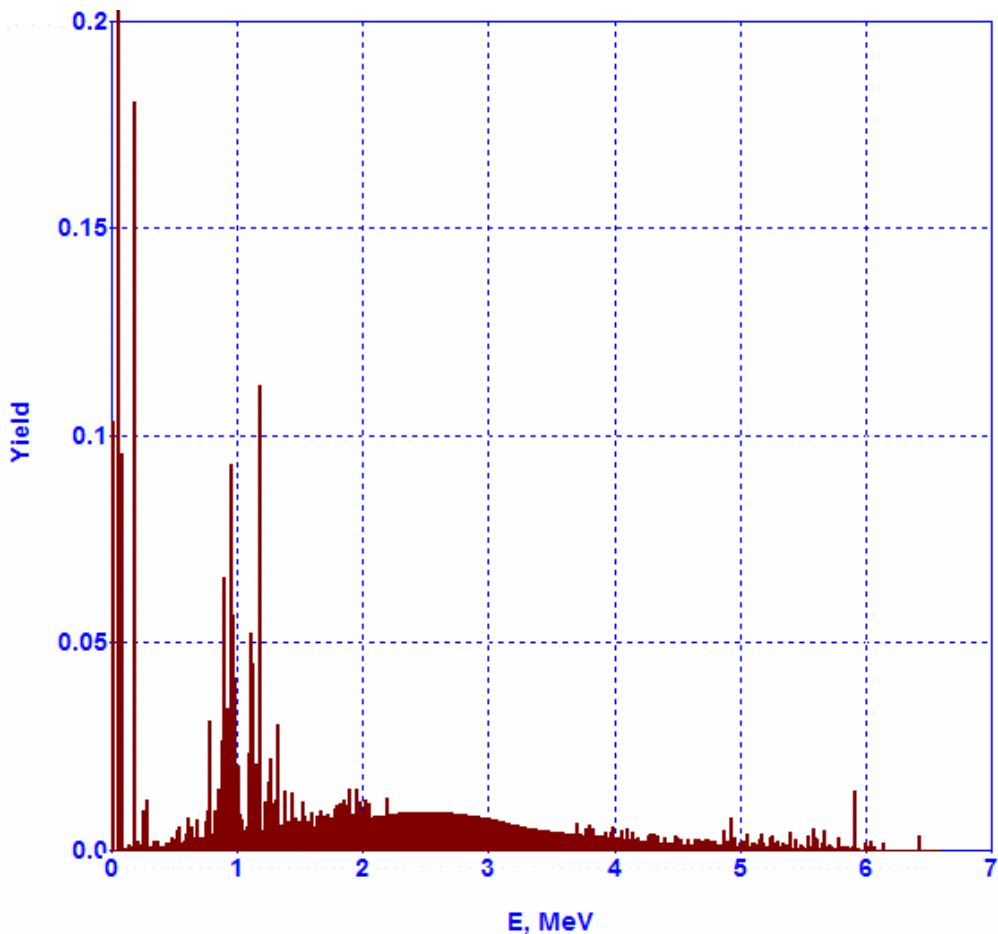


Fig. 13. Estimated photon spectrum (the reaction $^{157}\text{Gd}(n,\gamma)^{158}\text{Gd}$) (the axis of ordinates: number of photons in the interval 10 keV. Total energy of photon spectrum $E_\gamma = 7.87$ MeV. Yield = ~ 4)

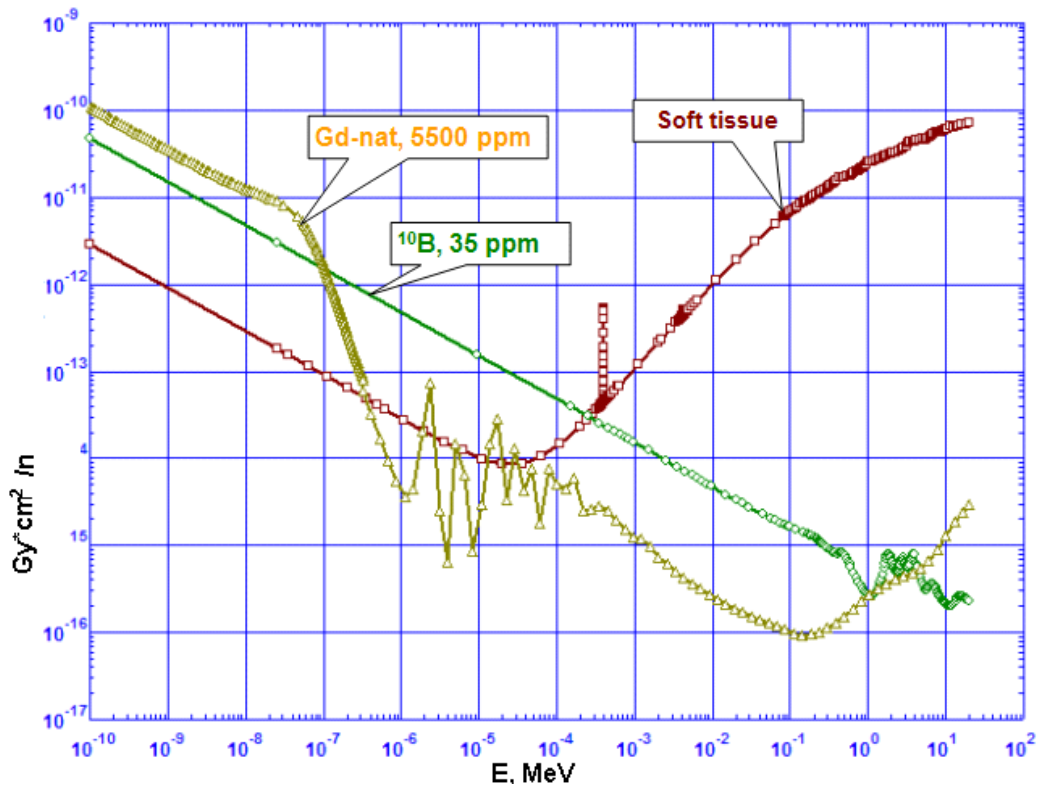


Fig. 14. Specific kerma of neutrons vs. energy for biological tissue (composition of elements corresponds to soft biological tissue) and neutron capture agents for their typical concentrations in the biological tissue.

Earlier it was considered that in case of gadolinium use, the basic damage of tumor cells is caused by the secondary photon radiation. However, our studies have shown: when gadolinium is localized in the tumor, the absorbed dose from electrons is comparable with the photon dose.

The intravenous Gd-containing drug Dipentast [17,18,19] is a new dosage form of gadopentetate, functionally similar to the intravenous compound Magnevist, but less toxic. Additionally, the composition includes adjuvant substance ensuring stability of the completed dosage form (water solution with pH ~7.5 [20]), and also having detoxifying properties, which has allowed to decrease the toxicity of the compound in comparison with the well-known drug Magnevist (Schering, Germany).

The structure of the complex obtained was confirmed by the method we developed earlier [20]. Essential attention was given to the pharmacokinetic study of the compound for the cases of different ways of administration to the organism. The selection of intramuscular and intratumoral administration is determined by the absence of specific accumulation of gadopentetate in tumor tissues that dictates the abovementioned ways of administration in the NCT technology.

Basic characteristics of the intravenous drug Dipentast: content of adjuvant substances - sodium gadopentetate - 290 ± 10 mg/ml; density of the solution at 20°C - $1.16 - 1.17$ g/cm³; viscosity at 20°C - 2.23 cp; constant of chelate stability, log K - 22.9 ; excretion - in urine.

The pharmacokinetic study of Dipentast was carried out using the method we developed, i.e. the neutron activation analysis (NAA) on the MEFH reactor. The studies were carried out in rats with inoculated sarcoma C-45.

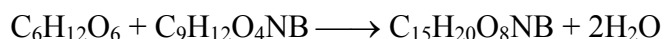
The technique of NAA on a vertical channel. The channel is installed in the thermal column of the reactor. The thermal neutron flux was 2.2×10^{11} n/cm²·s (the reactor power 2500 kW), and cadmium ratio on ¹⁹⁸Au = 400. Each sample was also irradiated for 5 minutes together with a neutron flux monitor made of an Mn-Al alloy. Five minutes later the samples were delivered to the measurement position. The duration of measurements on the gamma-spectrometer complex was 600 s. The limit of Gd detection with this technique is 1 µg.

The data fit with well-known fact and data of radioisotope studies of Dipentast [21]. The value $T_{1/2}$ of Dipentast from the tumors of animals is 3.0-3.5 times higher than that for Magnevist, with similar rates of drug elimination from the bloodstream.

Dipentast is being prepared for commercial production.

As the main ¹⁰B-compound, we used [¹⁰B]-L-boronphenylalanine in the form of borate ether with D-fructose (BPA) and D-galactose. [¹⁰B]-L-boronphenylalanine is manufactured by Katchem (Czech Republic) with a chemical purity of 98 % and enrichment in the isotope ¹⁰B of 99.7.

¹⁰B-L-phenylalanine interacts with hexoses in alkaline water solution by the same mechanism.



Borate ethers of ¹⁰B-L-phenylalanine with the hexoses D-fructose, D-galactose and D-glucose have identical element structure $\text{C}_{15}\text{H}_{20}\text{O}_8\text{NB}$ and identical molecular mass (MM = 412.348 g). On this basis, conformational thermodynamic analysis with use of the program HyperCem v.6.0 has been carried out. As a criterion of predominant formation of this or that structure, total energy of molecule formation has been chosen, taking into account only the formation of covalent connections. The energies of formation of charged structures (formation of —O—B—O— , —O—B(OH)—O— , —O—B(—O—)_2 , и —NH_3^+) were not calculated. The results of the analysis are shown in Table 1.

Table 1. Calculated energies of formation of borate ethers of monosaccharides with ^{10}B -boron-L-phenylalanine.

Monosaccharide	Form of the monosaccharide	Position of OH-groups participating in the borate ether formation, number of C atom	Calculated energy of borate ether formation, kcal/mole
α -D-galactose	galactopyranose	4,6	-57.594654
β -D- galactose	galactopyranose	4,6	-38.584030
α -D-fructose	fructofuranose	4,6	-22.794540
β -D- fructose	fructofuranose	4,6	-38.826360
α -D-glucose	glucopyranose	4,6	-37.783703
β -D- glucose	glucopyranose	4,6	-40.845066

The stereochemical factor appears to be determinative for the stability of borate ethers in water solution. So, borate ethers of D-galactose are stable in a more alkaline medium in comparison with similar derivatives of D-fructose. Results of the analysis comply with the literature on studying the reaction of BPA with D-fructose by the NMR method [22].

Concentrations of ^{10}B in biological tissues were determined using the track method. A film from cellulose acetobutyrate of 10 to 100 μm thick was used as the detector. The tracks were counted after etching the detector with sodium hydroxide solution and placing it under a microscope. A specially developed program was used for automated count of tracks from the digital camera pictures. The count of total number of tracks was performed over the detector area of 0.0025 mm^2 .

Researches are being performed with application of synthesized compounds: cobalt bis(dicarbollide) anion $[\text{3,3}'\text{-Co(1,2-C}_2\text{B}_9\text{H}_{11})_2]^-$ (CDA), δ -hydroxy- α -aminobutyric acid on the basis of cobalt bis(dicarbollide) anion $[\text{3,3}'\text{-Co(1,2-C}_2\text{B}_9\text{H}_{11})_2]$ (CDAA), and also a carborane derivative of estradiol (CE). CE is of interest for the administration of boron in hormone-dependent tumors. Research of CDA, CDAA and CE at the cellular level has started. It was shown on B-16 melanoma cell culture that the efficiency of CDA is not inferior to that of BPA.

Preclinical trials of the drugs Dipentast and dosage forms of BPA were carried out on cell cultures of melanoma B-16, sarcoma C-45, and also in small laboratory animals. Conditions were determined, under which the efficiency of treatment of experimental tumors in animals with use of the drugs Dipentast and BPA reaches 80 %.

Neutron capture agents containing Gd and ^{10}B atoms have different physical mechanisms of radiation damage on cells. It was interesting to estimate their mutual influence on the intensity of damage on tumor cells. A similar estimation was performed on a cell culture of murine melanoma.

The drugs were added into a cell suspension of murine melanoma, and then the suspension was irradiated with thermal neutron flux. The duration of neutron irradiation was chosen so that the colony growth rate and cell survival rate (primary criteria to estimate the therapeutic efficiency in NCT on a cell culture) were within the range of 30 - 50% under the condition of absence of a neutron capture drug in the suspension. It was shown that under the combined use of Dipentast and BPA, the suppression of colony growth rate and cell survival rate of B-16 is 4-6 times higher compared to the separate use of the specified drugs.

Pharmacokinetic studies

Pharmacokinetic studies are the basis for the development of irradiation planning systems in the NCT technology.

Dipentast and similar compounds are intercellular drugs [23]. The most acceptable way of administration for them is intratumoral (fig. 15). On the contrary, BPA is capable of penetrating into tumor cells. Both systemic and regional ways of administration are used for BPA.

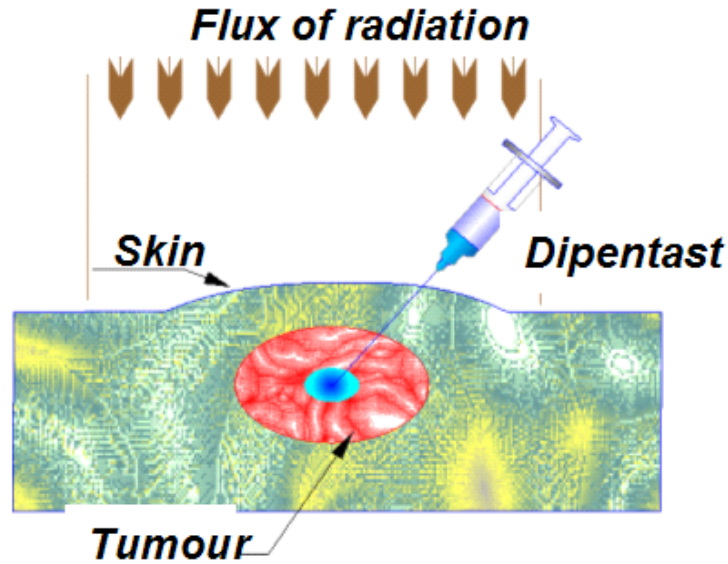


Fig. 15. Drug injection scheme.

Taking into account the pharmacological inertness of the drug Dipentast, the model of diffusion by C. Nicholson et al. [24] was taken as the basis of its pharmacokinetic model for the intratumoral administration.

In this case, the dynamics of spatial distribution of the drug concentration for a local administration of the volume V_0 of the drug solution of the mass M_0 at a depth of Z_0 will be the following:

$$C(r, t) = \frac{C_0}{2} \left\{ \operatorname{erf}\left(\frac{r + R_0}{\sqrt{4Dt}}\right) - \operatorname{erf}\left(\frac{r - R_0}{\sqrt{4Dt}}\right) + \frac{\sqrt{4Dt}}{r \cdot \sqrt{\pi}} \left(\exp\left(-\frac{(r + R_0)^2}{4Dt}\right) - \exp\left(-\frac{(r - R_0)^2}{4Dt}\right) \right) \right\}, \text{ g/cm}^3,$$

where $R_0 = \sqrt[3]{\frac{3V_0}{4\pi}}$; $r = \sqrt{x^2 + y^2 + (z - Z_0)^2}$.

The geometry of the calculation is shown in fig.16.

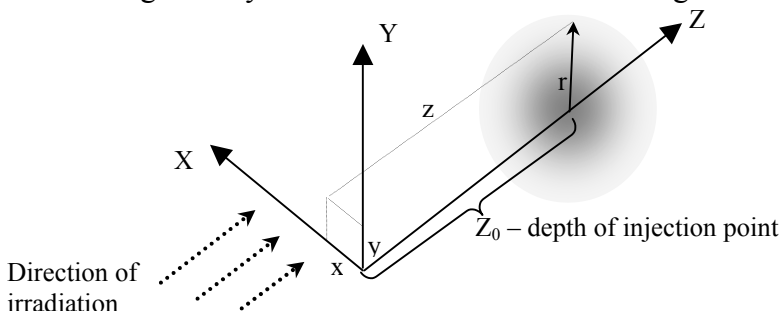


Fig.16. Calculation geometry.

The diffusion factor D is determined empirically basing on the data on the period of half elimination of the drug. For Dipentast, the diffusion factor obtained from the results of radioisotope studies $D = 0.58 \times 10^{-7} \text{ cm}^2/\text{s}$ appeared to be rather close to the values of the diffusion factor for complex polymers in the brain tissue [25]: PHPMA-BSA - $0.45 \times 10^{-7} \text{ cm}^2/\text{s}$; Dextran - $0.75 \times 10^{-7} \text{ cm}^2/\text{s}$.

Fig.17 shows the dynamics of spatial distribution of the drug Dipentast in biological tissue along the axis Z ($x=0, y=0$). The mass of Gd-DTPA = 0.0137 g. The volume of the drug solution administered = 0.1 cm^3 . Depth of injection = 2 cm.

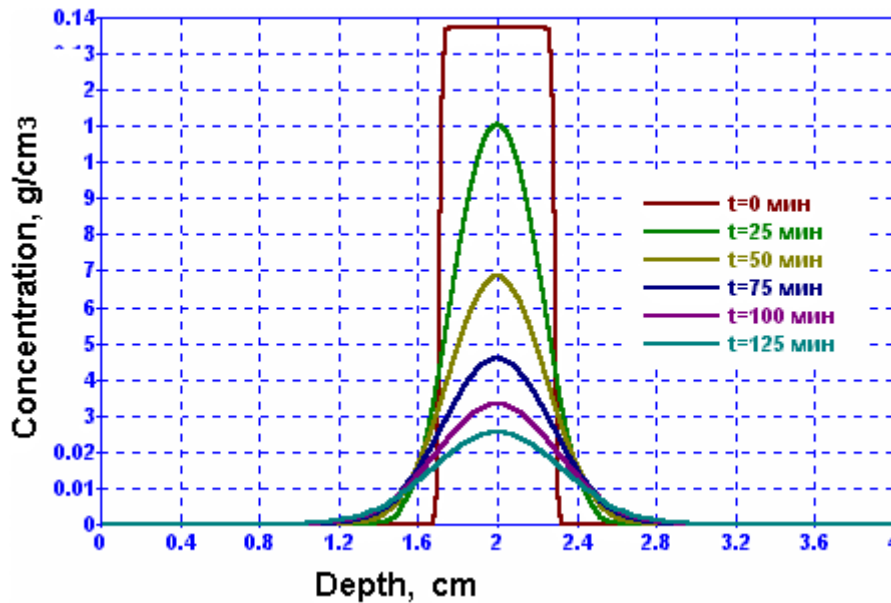


Fig 17. Distribution of Dipentast in biological tissue for various moments of time t .

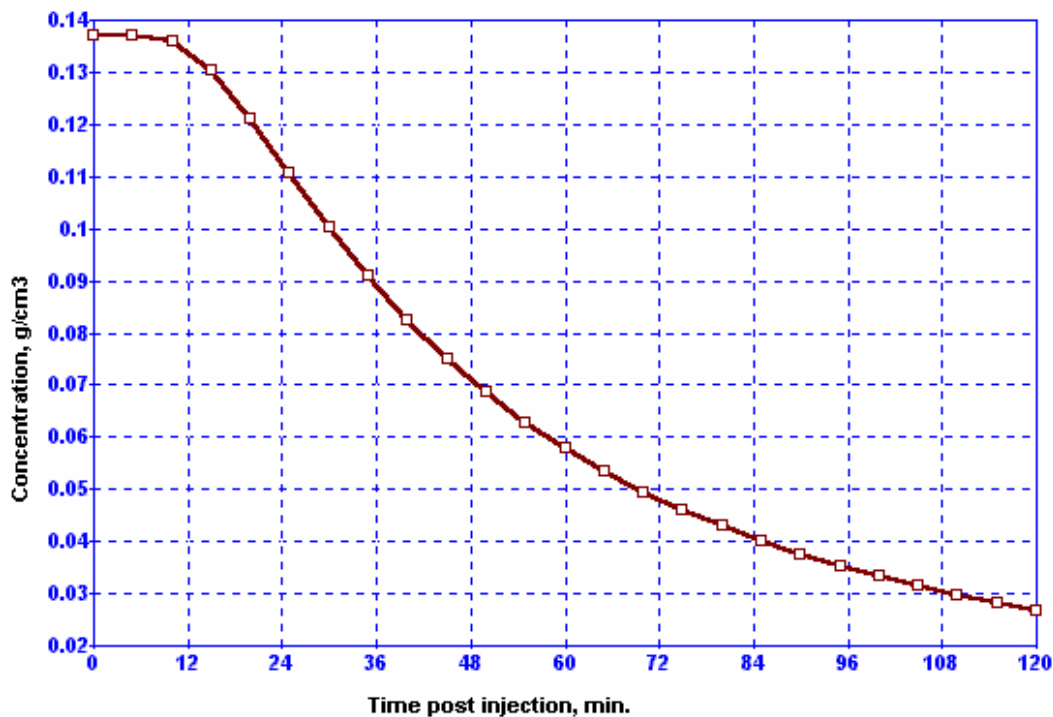


Fig. 18. Dynamics of Gd-complex concentration in the point of injection.

Fig. 18 shows the dynamics of the Gd-complex concentration calculated in the point of injection $Z=Z_0$.

The developed model agrees well with the experimental data, and can be the basis of a system of irradiation planning in GdNCT.

The main direction of our studies is development of a general mathematical model describing the migration of drugs in the organism taking into account the bloodstream intensity, parameters of blood and development of the capillary network in the pharmacological target for different ways of drugs administration to the organism.

Preclinical studies

Experimental clinical studies on the efficiency of boron neutron capture therapy (BNCT) of spontaneous melanoma in dogs with various phases of the cancer process were carried out. The following problems were being solved.

1. Work through the technique of irradiation of dogs with the neutron beam for subsequent preclinical approbation of the NCT method in large animal as a mandatory phase prior to the use of the method to treat oncological patients.
2. Estimate the efficiency of the neutron beam effect on normal tissues in the irradiation of dogs with melanoma (and without it) in respect to antitumor and side effects.
3. Select optimum irradiation time.

Prior to the NCT procedure, all dogs passed a complete clinical examination and peripheral blood test. Immediately prior to the irradiation session, the dogs were premedicated, which included subcutaneous administration of Atropinum and Sulfocamphocainum, and intramuscularly - Prednisolon, Kalipsol and Rometar. The anesthesia included intravenous administration of Kalipsolum, Rometar and Relanium. Relanium was used for the introductory narcosis, which favored deep narcotic sleep.

Detectors were placed on the body surface of the immobilized dog in order to register the dose of photon and neutron radiations. Also, melanoma B-16 cell suspension in plastic vials of 3 mm in diameter was used as a biological dosimeter.

During the irradiation time, the narcosis depth was maintained remotely by means of fractional intravenous administration of the anesthetic, and also the initial level of microcirculation was maintained using electrolytic solutions. The animals were under observation during the whole session of neutron irradiation with the help of a small video camera; the condition of the respiratory and cardiovascular systems was monitored, the respiration rate, blood pressure heart rate were recorded. After the irradiation, the animal was helped out of narcosis and transported to the clinic, where infusion therapy was applied to decrease the aftereffects of the long anesthesia.

The effect of irradiation was assessed visually; the changes of the condition of skin and subcutaneous fat were recorded. In order to determine the effect of irradiation on the hemopoiesis, peripheral blood tests were made in 3, 7, and 14 days, and also in 1, 3, and 6 months post irradiation.

On the basis of these experiments, the following conclusions were made:

1. The proposed method of anesthesia for the animal allows an NCT session of up to 2.5 hours.
2. The distinct spot of erythema confirms the immobility of the animal during the irradiation session, i.e. the fixation system backed with anesthesia allows irradiation of the tumor located close to critical tissues.
3. The irradiation session of up to 1.5 hours caused no significant changes of normal tissues and blood count.

4. The irradiation time of 1.5 hours corresponds to a thermal neutron fluence of $\sim 5 \times 10^{12}$ neutrons/cm².

Borate ethers of [¹⁰B]-L-boronphenylalanine with D-fructose and D-galactose were used as neutron capture compounds. The doses were 140 to 330 mg/kg (intravenously) and 50 to 200 mg/kg (regionally in the tumor-feeding) recalculated to boron-phenylalanine. The artery selection was monitored under X-rays with use of an X-ray contrast agent.

So far, 18 dogs have undergone NCT. The results of treatment can be estimated as positive.

Fig. 19 and 20 show dogs with spontaneous melanoma, prior to and post NCT treatment.

Efficiencies of BNCT, γ -therapy and radiotherapy on the neutron beam of the MEPhI reactor were compared. It was shown that lifetime of dogs with melanoma was 18 months post BNCT, 7 months after γ -therapy, and 6 months post neutron irradiation on the MEPhI reactor with no neutron capture drug.



Fig. 19. A dog with spontaneous melanoma on the outside of the upper lip: a) prior to irradiation, b) post irradiation.



Fig. 20. A dog with spontaneous melanoma on a foreleg (2 nodules): a) prior to irradiation, b) post irradiation.

Conclusions

The results obtained show the applicability of treatment of surface melanomas in the horizontal channel of the MEPhi reactor with use of borate ethers of L-boronphenylalanine with D-fructose and D-galactose.

The main obtained results were presented and published at the International Seminar in Capetown (1995), 8th International Symposium on NCT of Cancer in California (1998), 29th Conference of European Society for Radiation Biology in Capri (1998), 10th International Congress on NCT in Essen (2002).

Acknowledgements

The work has been carried out with financial support from Russian Fund for Technology Development of the Ministry of Science and Technologies of RF and International Science and Technology Center Project #1951.

References

1. *V.F. Khokhlov, P.N. Yashkin et al.* "Neutron Capture Therapy with Gadopentate Dimeglumine: Experiments on Tumor-Bearing Rats", "Academic Radiology" (USA), vol.2, 1995, p.392-398.
2. *V.F. Khokhlov, P.N. Yashkin, D.I. Silin, R. Lawaczek* "Neutron capture therapy with Gd-DTPA in tumor-bearing rats". Plenum Press, New York, 1996, p.865-869.
3. *V.F. Khokhlov, V.L. Gozenbuk, P.N. Yashkin, et al.* "Neutron capture therapy with Gd-complexes at the Moscow Research Thermal Reactor" 1997 Elsevier Science B.V. Advances in Neutron Capture Therapy. Vol.11, Chemistry and Biology. B.Larsson, J.Crawford and R.Weinreich, editors, p.447-450.
4. *V.F. Khokhlov, A.O. Korotkevich, T.S. Malutina, et al.* Biological evaluation of boron- and gadolinium-containing agents for NCT. Eighth International Symposium on Neutron Capture Therapy for Cancer. 13-18 September 1998, La Jolla, California, USA. Report E-94.
5. *V.F. Khokhlov, V.I. Bregadze, V.N. Koulakov, et al.* Development of boron- and gadolinium-containing compounds for net. Eighth International Symposium on Neutron Capture Therapy for Cancer. 13-18 September 1998, La Jolla, California, USA. Report P-5.
6. *V.F. Khokhlov, A.I. Shaks, V.L. Gozenbuk, et al.* Dose distribution in gadolinium containing phantoms subsequent to irradiation with thermal neutrons. Ibid, Report D-17.
7. *V.F. Khokhlov, V.N. Koulakov, K.N. Zailsev, et al.* Russian project for NCT of malignant tumours in humans. Ibid, Report Y-6.
8. *V.F. Khokhlov, A.O. Korotkevich, T.S. Malutina, et al.* Biological evaluation of boron- and gadolinium-containing agents for NCT. In: Application of neutrons in oncology: RI of Oncology TRC CO RAMS, - Tomsk, 1998., p. 16.
9. *J. Stepanek*, Radiation spectrum of ¹⁵⁸Gd and radial dose distribution. In Advances in Neutron Capture Therapy 2 (B. Larsson, J. Crawford and R. Weinreich, Eds.). Excerpta Medica, Int. Cong. Series 1132, Elsevier, Amsterdam, 1997.
10. *C. K. C Wang, M. Sutton, T. M. Evans and B. H. Laster*, A microdosimetric study of ¹⁰B(n,α)⁷Li and ¹⁵⁷Gd(n,γ) reactions for neutron capture therapy. In Proceedings of the Sixth International Radiopharmaceutical Dosimetry Symposium (A. T. Stelsen, M. G. Stabin and R. B. Sparks, Eds.), pp. 336–344. Report ORISE 99-0164, Oak Ridge Institute for Science and Education, Oak Ridge, TN, 1999.
11. *Tim Goorley, Hooshang Nikjoo*, Electron and Photon Spectra for Three Gadolinium-Based Cancer Therapy Approaches. Radiat. Res. 54, 556–563 (2000).
12. *J. K. Tuli*, Evaluated Nuclear Data File. Report BNL-NCS-51655-Rev. 87, Brookhaven National Laboratory, Upton, NY, 1987.
13. *L.V.Groshev, A.M.Demidov, V.N.Lutsenko, V.I.Pelekhov*, Атлас спектров гамма-лучей радиационного захвата тепловых нейтронов. Atlas of spectra of gamma-rays from radiation capture of thermal neutrons. – M: Atomizdat, 1958. - 111 p.

14. *J.T. Goorley, W.S. Kiger III, and R.G. Zamenhof*, "Reference Dosimetry Calculations for Neutron Capture Therapy with Comparison of Analytical and Voxel Models," *Medical Physics*, January 2002.
15. *Y.Mishima*, Melanoma and Non-melanoma neutron capture therapy using gene therapy: overview. In: *Advances in neutron capture therapy*. Larsson B, Crawford J, Weinreich R, eds. Elsevier Science, Amsterdam (1996) p. 10-25
16. Patent of Russian Federation № 2150961 from 06.02.98.
17. *V.N.Kulakov, V.I.Bregadze, et al.*, 2001. Design of Boron- and Gadolinium-containing Agents for NCT, In: M. F. Hawthorne, K.Shelly, R.J.Wiersema *Frontiers in Neutron Capture Therapy*, Kluwer Academic/Plenum Publishers, New York, Vol.2, pp 843-846.
18. *Kulakov, V.N., V.F.Khokhlov et al.*, Compounds with ^{10}B and Gd in the Russian NCT Project, *Research and Development in NCT*, Essen, September 8-13 2002, Ed.: W.Sauerwein, R.Moss, A.Wittig, Monduzzi Editore, Intern. Proceeding Division, 2002, p. 107-109.
19. *L.G.Shpinkova, V.N.Kulakov et al.* Stability of ^{111}In -ligand Complexes. Studied by TDPAC, *Z. Naturforsch.*, b. 53a, s. 630-635, 1998.
20. *V.F.Khokhlov, K.N.Zaitsev, V.I.Kvasov et al.*, Development of a radiation technology to treat malignant tumors on the base of NCT, *Engineering Physics (Rus.)*, № 1, 2000, p. 52-55.
21. *B.K.Shull, D.E.Spielvogel, et al.*, Evidence for spontaneous, reversible paracyclophane formation. Aprotic solution structure of the boron neutron capture therapy drug, L-*p*-boronphenylalanine, *J. hem. Soc., Perkin Trans.*, v. 2, 2000, p. 557-561.
22. *R.Felix, A.Heshiki, N.Hosten, H.Hricak*, *Magnevist*, Oxford, Blackwell Scientific Publication, 1994, 192 p.
23. *C. Nicholson* Diffusion from an injected volume of substance in brain tissue with arbitrary volume fraction and tortuosity. *Brain Res.* 333:325-329, 1985
24. *S. Prokopova-Kubinova, L.Vargova. L.Tao, C. Nicholson et al.* Poly[N-(2-hydroxypropyl)methacrylamide] Polymers Diffuse in Brain Extracellular Space with Same Tortuosity as Small Molecules. *Biophysical Journal*, Volume 80, January 2001, 542-548.